Hybrid Modulation Formats Enabling Elastic Fixed-Grid Optical Networks

Fernando P. Guiomar, *Member, OSA,* Rixin Li, Chris R. S. Fludger, *Member, IEEE, Member, OSA,* Andrea Carena, *Member, IEEE,* and Vittorio Curri, *Member, IEEE*

***Abstract*—In this paper, we analyze hybrid modulation formats as an effective technology for the implementation of flexible transponders that are capable of trading-off the delivered data rate by the lightpath quality of transmission with fine granularity. Flexible transponders are an enabling technology to introduce the elastic paradigm in state-of-the-art networks, while maintaining compatibility with the installed equipment, including fibers, mux-demux and ROADMs, as required by telecom operators willing to exploit fixed-grid WDM transmission. We consider two solutions achieving different levels of flexibility and employing different hybridization approaches: time-division (TDHMF) and quadrature-division (Flex-PAM) hybrid modulation formats. We introduce a comprehensive theoretical assessment of back-to-back performances, analyzing different transmitter operating conditions, and we provide an extensive simulation analysis on the propagation of a Nyquist-WDM channel comb over an uncompensated and amplified fiber link. After assessing the impact of nonlinear propagation on the maximum signal reach, we present simple countermeasures for nonlinear mitigation and discuss on their effectiveness for both TDHMF and Flex-PAM.**

***Index Terms*—Flexible transponders, hybrid formats, GN-model, elastic networks.**

I. Introduction

THE exponential growth of IP traffic [1] together with an increased level of traffic fluctuations drives the need for highly efficient and flexible broadband networks, starting from optical back-bones. Optical networks are evolving towards flexibility, with the purpose of maximizing the data-rate and reach by adapting their operation to the traffic demand. From the point of view of telecommunications carriers, there is a firm requirement to have a return on capex investments for the installed infrastructures, aiming at solutions avoiding replacement of equipments and fibers [2]. Consequently, carriers plan to keep fixed-grid DWDM transmission on the installed equipment, introducing network efficiency and flexibility through the replacement of transponders. This network evolution based on installed links envisions to maintain the channel spacing, Δf, and the symbol rate, R_s, as constant parameters, given by the transmitter (Tx) and receiver (Rx) state-of-the-art.

Thanks to the introduction of fast digital signal processing (DSP) at the Tx/Rx, flexible transponders with the capability to switch among polarization-multiplexed (PM) multilevel modulation formats are now available on the market. They enable network flexibility allowing to trade-off data-rate with the lightpath quality of transmission (QoT), i.e., with the optical signal-to-noise ratio (OSNR). But such data-rate flexibility is limited to the cardinality of the selected modulation formats. For instance, if we consider a transponder able to switch among PM-QPSK, PM-16QAM, and PM-64QAM, delivering 4, 8, and 12 bit-per-symbol (BpS), respectively, the available data-rates, given the symbol rate R_s, are only the three values $R_b = R_s \cdot BpS$. An increased flexibility could be achieved by using cross-QAM constellations, such as PM-8QAM and PM-32QAM [3]. However, on the contrary of square QAM, these non-rectangular constellations do not support perfect Gray coding and also do not allow to easily modulate and demodulate the in-phase and quadrature components as independent pulse amplitude modulation (PAM) signals. This may be an important disadvantage for a flexible transceiver supporting several modulation formats, as it requires the co-existence of radically different modulation and demodulation stages.

Targeting an enhanced data-rate flexibility, a plethora of enabling techniques for the implementation of flexible transponders have been recently proposed, such as 4D-optimized modulation formats [4], [5], coded modulation [6], [7] and rate-adaptive modulation [8]. Besides the aforementioned techniques, the use of hybrid modulation formats has also been attracting significant attention [9]–[20] introducing the ability to trade-off with fine granularity the data-rate with the QoT. These are based on mixing different constellations in order to deliver fractional values of BpS. The hybridization can be done with respect to time, generating the time-division hybrid modulation formats (TDHMF), which have been extensively assessed both in simulation [9]–[11] and experimental works [12]–[18], [21]. Alternatively, it is also possible to hybridize with respect to the four quadratures (I_x, Q_x, I_y, Q_y), generating the flexible pulse-amplitude modulation (Flex-PAM) concept [19], [20]. Although providing a limited bit-rate granularity with respect to TDHMF, Flex-PAM resorts only to time-invariant *rectangular*[1] QAM constellations, thereby facilitating the modulation and demodulation stages, which are always based on the assignment of independent PAM signals to each quadrature.

In this paper, we provide a comprehensive theoretical and numerical comparison of TDHMF and Flex-PAM, both

F. Guiomar, Rixin Li, A. Carena, and V. Curri are with the Department of Electronics and Telecommunications, Politecnico di Torino, Torino, Italy. Website: www.optcom.polito.it e-mail: curri@polito.it. C. R. S. Flugder is with Cisco Optical GmbH, Nuremberg 90411, Germany. e-mail: cfludge@cisco.com.

[1]Note that, on the contrary of typical rectangular QAM, the Flex-PAM concept allows for different Euclidean distances in the in-phase and quadrature components. See section II.C for further details.

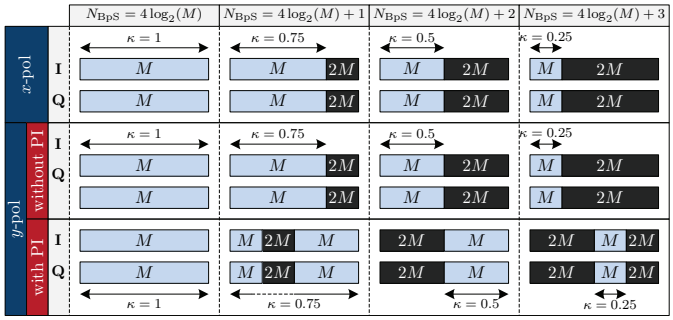

Fig. 1. Structure of a dual-polarization TDHMF frame composed of two square QAM modulation formats of size M^2 and $(2M)^2$. Envisioning an improved nonlinear propagation performance, polarization interleaving can be applied to balance the distribution of optical power over time. For simplicity, only frame structures that lead to integer number of bits per symbol are illustrated.

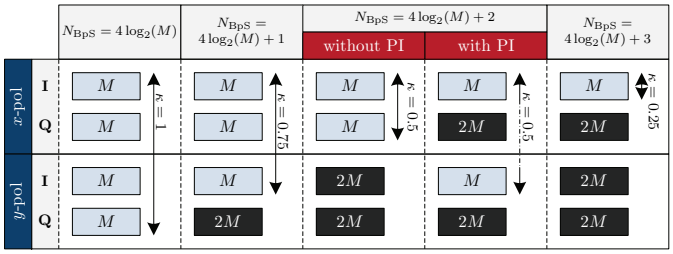

Fig. 2. Structure of a dual-polarization Flex-PAM frame composed of PAM modulation formats of size M and $2M$. Polarization interleaving can only be applied for $\kappa = 0.5$, enabling to balance the distribution of optical power between the two polarizations. Note that Flex-PAM inherently only allows for integer number of bits per symbol.

in terms of back-to-back (B2B) and signal propagation performance, targeting a flexible but low-complexity transponder architecture. The main performance-limiting aspects of TDHMF and Flex-PAM due to fiber nonlinearities are discussed and appropriate countermeasures are presented and numerically assessed in a Nyquist-WDM scenario comprising a wide range of channel bit-rates.

The remainder of this paper is organized as follows. In Section II, we start by theoretically assessing the B2B performances of both TDHMF and Flex-PAM modulation formats, then reviewing different transmitter operation modes and devising the main B2B aspects to be taken into account for signal propagation. In Section III, we present a comprehensive simulative analysis of nonlinear propagation of a Nyquist-WDM channel comb over an uncompensated amplified link, deriving the maximum reach for a large set of conditions. To mitigate the nonlinear propagation impact we assess two techniques, polarization interleaving and power-ratio tuning, discussing on their effectiveness. A final comparison of maximum reach performances with the Gaussian noise (GN) model [22] predictions, used here as a reference, shows that both TDHMF and Flex-PAM present minor penalties when nonlinear mitigation techniques are used.

II. Theoretical Formulation

A. Time Domain Hybrid Modulation Formats

The general structure of a dual-polarization TDHMF frame is illustrated in Fig. 1, where for simplicity we only depict the configurations leading to an integer number of bits per symbol. In order to reduce the complexity associated with the transmission and detection of TDHMF, in this work we will consider that each periodic frame is composed of N symbols distributed among two neighbor square QAM modulation formats with constellation sizes M^2 and $(2M)^2$, where M is the number of levels in each quadrature. The TDHMF frame is also characterized by a given frame ratio, $\kappa = N_1/N$, where N_1 represents the number of symbols occupied by the modulation format with the lowest constellation size, M^2. In order to counteract the detrimental impact of time-varying optical power on the signal propagation performance [11], in the schematic representation of Fig. 1 we also illustrate the application of polarization interleaving (PI), which only changes frame layout in one polarization tributary, thus balancing optical power evolution over time. Nevertheless, from a B2B perspective, note that PI produces no impact on the performance of TDHMF, since the two polarization tributaries are completely orthogonal.

In order to analyze the B2B performance of TDHMF, we make use of the analytical estimation of the bit error rate (BER) for an M^2-QAM modulation format [23], whose expression is:

$$\Psi_{\mathrm{QAM}}(\mathrm{SNR}, M) = \frac{M-1}{M\log_2(M)}\mathrm{erfc}\left(\sqrt{\frac{3\,\mathrm{SNR}}{2(M^2-1)}}\right), \quad (1)$$

where SNR is the signal-to-noise ratio (SNR) per symbol and $\mathrm{erfc}(\cdot)$ is the complementary error function defined as,

$$\mathrm{erfc}(x) = \frac{2}{\sqrt{\pi}}\int_x^\infty e^{-t^2}dt. \quad (2)$$

Taking into account the characteristic frame-ratio, κ, and constellation size, M^2, the average BER of the TDHMF frame can then be written as,

$$\Psi_{\mathrm{TDHMF}}(\mathrm{SNR}_{\mathrm{QAM},1}, \mathrm{SNR}_{\mathrm{QAM},2}, M, \kappa) = \frac{4}{N_{\mathrm{BpS}}}\Big[\kappa\log_2(M)\Psi_{\mathrm{QAM}}(\mathrm{SNR}_{\mathrm{QAM},1}, M) + (1-\kappa)(\log_2(M)+1)\Psi_{\mathrm{QAM}}(\mathrm{SNR}_{\mathrm{QAM},2}, 2M)\Big], \quad (3)$$

where N_{BpS} is the average number of bits per symbol encoded in the TDHMF frame,

$$N_{\mathrm{BpS}} = 4\left(\log_2(M) + 1 - \kappa\right), \quad (4)$$

and $\mathrm{SNR}_{\mathrm{QAM},1}$, $\mathrm{SNR}_{\mathrm{QAM},2}$ represent the SNR perceived by each QAM format, determining the average SNR for the TDHMF frame, $\overline{\mathrm{SNR}}_{\mathrm{TDHMF}}$, which is given by,

$$\overline{\mathrm{SNR}}_{\mathrm{TDHMF}} = \kappa\mathrm{SNR}_{\mathrm{QAM},1} + (1-\kappa)\mathrm{SNR}_{\mathrm{QAM},2}. \quad (5)$$

In general, we can define a given power-ratio, PR, between the two modulation formats such that,

$$\mathrm{PR}\ [dB] = 10\log_{10}\left(\frac{\mathrm{SNR}_{\mathrm{QAM},1}}{\mathrm{SNR}_{\mathrm{QAM},2}}\right). \quad (6)$$

The power-ratio will depend on the adopted transmitter operation strategy and will set the B2B performance of TDHMF.

B. Flex-PAM

As an alternative flexible modulation scheme, in Fig. 2 we show the proposed dual-polarization Flex-PAM frame structure. As opposed to TDHMF, Flex-PAM does not imply time-varying modulation. Instead, the flexibility is achieved through the hybridization of PAM formats between the four orthogonal quadratures (in-phase and quadrature in the two polarizations). Consequently, the granularity of Flex-PAM is inherently limited to integer numbers of bits per symbol. Similarly to the TDHMF case, in this work we will consider that the Flex-PAM frame is composed of two nearest-size PAM formats, whose constellations include M and $2M$ symbols, respectively. Under these assumptions, the Flex-PAM frame can be completely described by the number of levels of its lowest size PAM format, M, and by the corresponding frame-ratio, κ.

Similarly to TDHMF, PI can also be applied to reduce the optical power unbalance between the two polarizations. However, PI is only possible in Flex-PAM for $\kappa = 0.5$, as shown in Fig. 2. For the remaining frame-ratios it is not possible to rearrange the frame structure in order to balance the optical power between polarizations. Other advanced methodologies must be applied, as it will be discussed in Section III. In order to unequivocally identify the frame structure when using PI, the Flex-PAM format can be identified by a vector $\overline{\overline{\mathbf{M}}} = [M_1,\ M_2,\ M_3,\ M_4]$, where M_i represents the number of PAM levels in each quadrature, such that $M = \min\left(\overline{\overline{\mathbf{M}}}\right)$.

To analyze the B2B performance of Flex-PAM we may use the BER estimation expression of an M-PAM modulation format [23],

$$\Psi_{\text{PAM}}(\text{SNR}, M) = \frac{M-1}{M\log_2(M)}\text{erfc}\left(\sqrt{\frac{3\,\text{SNR}}{M^2-1}}\right). \quad (7)$$

Starting from (7), the overall BER of a Flex-PAM frame can be estimated by individually accounting for the BER incurred in each of its four orthogonal quadratures as,

$$\begin{aligned}\Psi_{\text{Flex-PAM}}(\text{SNR}_{\text{PAM},1}, \text{SNR}_{\text{PAM},2}, M, \kappa) = \\ \frac{4}{N_{\text{BpS}}}\Big[\kappa\log_2(M)\Psi_{\text{PAM}}(\text{SNR}_{\text{PAM},1}, M) \\ +(1-\kappa)(\log_2(M)+1)\Psi_{\text{PAM}}(\text{SNR}_{\text{PAM},2}, 2M)\Big],\end{aligned} \quad (8)$$

where the N_{BpS} is given by expression (4).

Similarly to the TDHMF case, the average SNR is given by,

$$\overline{\text{SNR}}_{\text{Flex}-\text{PAM}} = \kappa\text{SNR}_{\text{PAM},1} + (1-\kappa)\text{SNR}_{\text{PAM},2}, \quad (9)$$

with $\text{SNR}_{\text{PAM},1}$ and $\text{SNR}_{\text{PAM},2}$ now corresponding to the SNR locally perceived by each PAM format in a single quadrature, as opposed to (5), where $\text{SNR}_{\text{QAM},1}$, $\text{SNR}_{\text{QAM},2}$ are measured over both in-phase and quadrature. Since the noise power is set by the propagation channel but the signal power of M^2-QAM is twice of that of M-PAM, then it results that for the same M,

$$\overline{\text{SNR}}_{\text{QAM}} = 2\cdot\overline{\text{SNR}}_{\text{PAM}}. \quad (10)$$

Note that the factor of 2 in expression (10) compensates for the factor of 2 between denominators in the arguments of the $\text{erfc}(\cdot)$ functions of expressions (1) and (7). Consequently, the B2B performance of both strategies is exactly equivalent. In the following, we provide further details on possible transmitter operation strategies for Flex-PAM, which can also be equivalently applied to TDHMF. For the compactness of notation, henceforth we will refer to $\text{SNR}_{\text{PAM},1}$, $\text{SNR}_{\text{PAM},2}$ and $\overline{\text{SNR}}_{\text{PAM}}$ simply as SNR_1, SNR_2 and $\overline{\text{SNR}}$.

C. Transmitter Operation Strategies

In this section we present different transmitter operation strategies analyzed on a per-channel basis, using the average BER of the hybrid format as the performance criterion.

1) Constant Power ($\text{PR}=0$ dB): If the power is kept constant for both PAM modulations composing the Flex-PAM, then the power ratio between formats is $\text{PR} = 0$ dB and the SNR perceived by each format is $\text{SNR}_1 = \text{SNR}_2 = \overline{\text{SNR}}$. Using equation (8) we obtain the following BER expression,

$$\begin{aligned}\Psi = &\frac{1}{M\left(\log_2(M)+1-\kappa\right)}\Bigg[\kappa(M-1)\,\text{erfc}\left(\sqrt{\frac{3\,\overline{\text{SNR}}}{M^2-1}}\right) \\ &+(1-\kappa)\left(M-\frac{1}{2}\right)\text{erfc}\left(\sqrt{\frac{3\,\overline{\text{SNR}}}{4M^2-1}}\right)\Bigg].\end{aligned} \quad (11)$$

This is the simplest transmitter operation strategy, but, as we are going to discuss in the following, it is inefficient both in terms of performance (large B2B penalties) and receiver-side complexity, since the two PAM/QAM formats operate at completely different BERs, thus requiring dedicated forward-error correction (FEC) codes.

2) Same Euclidean Distance ($d_1 = d_2$): In order to guarantee the same Euclidean distance, d_1 and d_2, between the two modulation formats in the Flex-PAM frame, it can be shown that SNR perceived by each of the PAM formats is respectively given by,

$$\text{SNR}_1 = \frac{M^2-1}{(4-3\kappa)M^2-1}\,\overline{\text{SNR}}, \quad (12)$$

and

$$\text{SNR}_2 = \frac{4M^2-1}{(4-3\kappa)M^2-1}\,\overline{\text{SNR}}. \quad (13)$$

Substituting (12) and (13) into the BER expression (8) and reducing all its terms as functions of $\overline{\text{SNR}}$, M and κ yields,

$$\Psi = \frac{M-\frac{\kappa+1}{2}}{M\left(\log_2(M)+1-\kappa\right)}\,\text{erfc}\left(\sqrt{\frac{3\,\overline{\text{SNR}}}{(4-3\kappa)M^2-1}}\right). \quad (14)$$

The associated power-ratio between the two PAM formats is then given by,

$$\text{PR} = 10\log_{10}\left(\frac{4M^2-1}{M^2-1}\right), \quad (15)$$

TABLE I
FLEX-PAM FRAME STRUCTURE, POWER-RATIO AND REQUIRED SNR FOR DIFFERENT TRANSMITTER OPERATION STRATEGIES, CONSIDERING A TARGET BER OF 2×10^{-2}

N_{BpS}	$\log_2\left(\overline{\overline{\mathbf{M}}}\right)$	Format	M	κ	$d_1 = d_2$			$\Psi_1 = \Psi_2$			$\Psi_{\min}$		
					$\mathrm{SNR}_{\mathrm{req}}$ [dB]	PR [dB]	$\mathrm{PR}_{\mathrm{pol}}$ [dB]	$\mathrm{SNR}_{\mathrm{req}}$ [dB]	PR [dB]	$\mathrm{PR}_{\mathrm{pol}}$ [dB]	$\mathrm{SNR}_{\mathrm{req}}$ [dB]	PR [dB]	$\mathrm{PR}_{\mathrm{pol}}$ [dB]
4	[1 1 1 1]	PM-QPSK	2	1	6.25	0	0	6.25	0	0	6.25	0	0
5	[1 1 1 2]		2	0.75	9.07	7	4.78	8.94	6.46	4.33	8.76	4.87	3.08
6	[1 2 1 2]	PM-8QAM[1]	2	0.5	10.69	7	0	10.59	6.46	0	10.46	5	0
7	[1 2 2 2]		2	0.25	11.83	7	2.22	11.78	6.46	2.13	11.72	5.09	1.84
8	[2 2 2 2]	PM-16QAM	4	1	12.71	0	0	12.71	0	0	12.71	0	0
9	[2 2 2 3]		4	0.75	15.11	6.23	4.15	14.98	5.72	3.74	14.72	3.69	2.23
10	[2 3 2 3]	PM-32QAM[1]	4	0.5	16.57	6.23	0	16.45	5.72	0	16.25	3.9	0
11	[2 3 3 3]		4	0.25	17.62	6.23	2.08	17.56	5.72	1.98	17.45	4.04	1.57
12	[3 3 3 3]	PM-64QAM	8	1	18.43	0	0	18.43	0	0	18.43	0	0

imposing a maximum value of ∼7 dB for $M = 2$ and asymptotically converging to ∼6 dB when increasing M.

3) Same BER ($\Psi_1 = \Psi_2$): In order to impose that the two modulation formats in the Flex-PAM frame must operate at the same BER, we must determine the SNR required by each format to achieve the target BER, Ψ_{target}, which can be obtained by inverting the BER expression (7),

$$\mathrm{SNR}_1^{\mathrm{req}} = \frac{M^2-1}{3}\,\mathrm{erfc}^{-1}\left(\frac{M\log_2(M)}{M-1}\Psi_{\mathrm{target}}\right)^2, \quad (16)$$

and

$$\mathrm{SNR}_2^{\mathrm{req}} = \frac{4M^2-1}{3}\,\mathrm{erfc}^{-1}\left(\frac{2M(\log_2(M)+1)}{2M-1}\Psi_{\mathrm{target}}\right)^2. \quad (17)$$

The average BER of the entire frame is then obviously given by Ψ_{target}, whereas the average SNR is obtained by substituting $\mathrm{SNR}_1^{\mathrm{req}}$ and $\mathrm{SNR}_2^{\mathrm{req}}$ in (9). Finally, the power-ratio between PAM formats is given by,

$$\mathrm{PR} = 10\log_{10}\left(\frac{\mathrm{SNR}_1^{\mathrm{req}}}{\mathrm{SNR}_2^{\mathrm{req}}}\right). \quad (18)$$

4) Minimum BER ($\Psi_{\min}$): To achieve the minimum global BER requires to find the optimum SNR pair, $[\mathrm{SNR}_1^{\mathrm{opt}}, \mathrm{SNR}_2^{\mathrm{opt}}]$, that minimizes the estimated BER of expression (8). Taking into account that for any given $\overline{\mathrm{SNR}}$ the value of SNR_2 is automatically determined by the value of SNR_1 through expression (9), the following optimization procedure can be applied to determine $\mathrm{SNR}_1^{\mathrm{opt}}$,

$$\mathrm{SNR}_1^{\mathrm{opt}} = \left\{\mathrm{SNR}_1 : \Psi_{\text{Flex-PAM}}\left(\mathrm{SNR}_1, \frac{\overline{\mathrm{SNR}}-\kappa\mathrm{SNR}_1}{1-\kappa}, M\right)\right.$$
$$\left. = \min\left[\Psi_{\text{Flex-PAM}}\left(\mathrm{SNR}_1, \frac{\overline{\mathrm{SNR}}-\kappa\mathrm{SNR}_1}{1-\kappa}, M\right)\right]\right\}, \quad (19)$$

whereas $\mathrm{SNR}_2^{\mathrm{opt}}$ is given by,

$$\mathrm{SNR}_2^{\mathrm{opt}} = \frac{\overline{\mathrm{SNR}}-\kappa\mathrm{SNR}_1^{\mathrm{opt}}}{1-\kappa}. \quad (20)$$

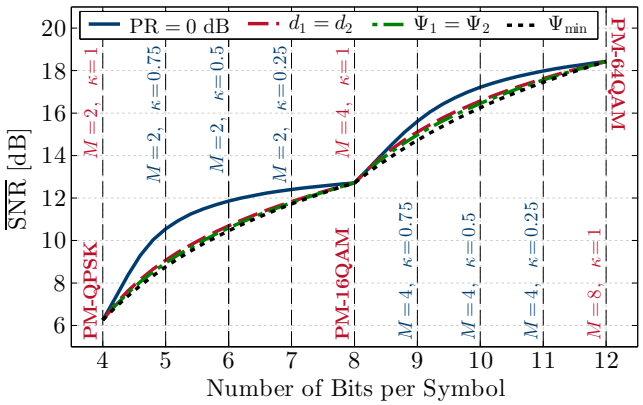

Fig. 3. Back-to-back sensitivity of TDHMF depending on the transmitter operation strategy for a number of bits per symbol ranging from 4 (PM-QPSK) up to 12 (PM-64QAM). Note that the sensitivity of Flex-PAM coincides with that of TDHMF for integer N_{BpS}. The target BER is 2×10^{-2}.

The average BER of the entire frame is then given by,

$$\Psi = \frac{1}{M\left(\log_2(M)+1-\kappa\right)}\left[\kappa(M-1)\,\mathrm{erfc}\left(\sqrt{\frac{3\,\mathrm{SNR}_1^{\mathrm{opt}}}{M^2-1}}\right)\right.$$
$$\left. + (1-\kappa)\left(M-\frac{1}{2}\right)\mathrm{erfc}\left(\sqrt{\frac{3\,\mathrm{SNR}_2^{\mathrm{opt}}}{4M^2-1}}\right)\right]. \quad (21)$$

As for the $\Psi_1 = \Psi_2$ strategy, the power-ratio between PAM formats is given by,

$$\mathrm{PR} = 10\log_{10}\left(\frac{\mathrm{SNR}_1^{\mathrm{opt}}}{\mathrm{SNR}_2^{\mathrm{opt}}}\right). \quad (22)$$

D. Back-to-Back Performance

Employing the previously described transmitter operation strategies and BER estimation formulas, the theoretical B2B sensitivity of TDHMF and Flex-PAM is shown in Fig. 3, in terms of required average SNR to achieve a given number of bits per symbol, ranging from 4 (*pure* PM-QPSK) up to

[1]Note that the PM-8QAM and PM-32QAM formats indicated in Table I are non-square (rectangular) QAM formats.

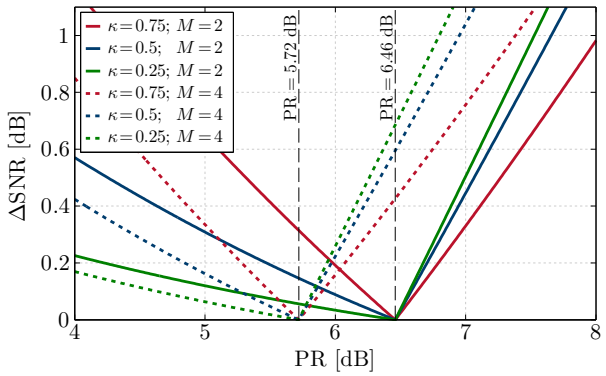

Fig. 4. SNR penalty (ΔSNR) incurred in B2B by tuning the power-ratio around its optimum value using the $\Psi_1 = \Psi_2$ transmitter operation strategy. The target BER is 2×10^{-2}.

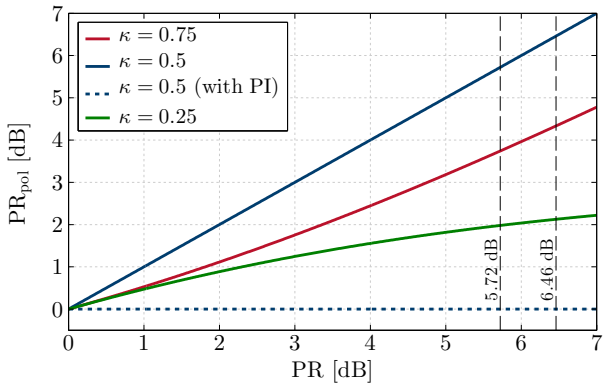

Fig. 5. Flex-PAM: impact of PR tuning on the power unbalance between polarization tributaries (or equivalently, the polarization power-ratio $\mathrm{PR_{pol}}$).

12 (*pure* PM-64QAM). Note that, as previously highlighted, TDHMF and Flex-PAM are equivalent in terms of sensitivity for integer number of bits per symbol. Complementarily to the sensitivity analysis of Fig. 3, the frame structure, power-ratio and required SNR of Flex-PAM is detailed in Table I for the same range of bits per symbol. Since it can play a key role on the signal performance after nonlinear fiber propagation, besides the power-ratio between PAM formats, Table I also indicates the correspondent power-ratio between polarization tributaries, $\mathrm{PR_{pol}}$. It is defined as the power-ratio between the y-pol (highest power polarization, according to Fig. 2) and the x-pol. Note that, for square ($\kappa = 1$) and rectangular ($\kappa = 0.5$) QAM constellations the polarization power-ratio is always 0 dB, whereas it is highest for $\kappa = 0.75$.

It is also important to emphasize that, apart from the $\mathrm{PR} = 0$ dB strategy, which is clearly sub-optimal, the remaining operation strategies are nearly equivalent in terms of sensitivity. Although the $\Psi_{\min}$ operation provides up to ~ 0.25 dB improved sensitivity for the considered range of bits per symbol, the $\Psi_1 = \Psi_2$ strategy is the most conservative approach: both formats operate at the same BER facilitating the FEC coding and decoding. Based on this observation, we are going to focus on the same BER transmitter operation strategy for the remainder of this paper. However, this strategy implies that, whenever the BERs of the two modulation formats are not exactly the same (e.g., due to PR mismatch in B2B or due to nonlinear phenomena after signal propagation in fiber), the system performance is limited by the highest BER.

To provide a more in-depth analysis of the consequences of adopting the same BER operating strategy, in Fig. 4 we show the SNR penalty, ΔSNR, incurred by sweeping the power-ratio between formats. Indeed, the optimum performance ($\Delta\mathrm{SNR} = 0$ dB) is obtained at the theoretical values listed in Table I, 6.46 dB for $M = 2$ and 5.72 dB for $M = 4$. It is also important to notice that the slope of the curves in Fig. 4 strongly depends on the frame-ratio, κ. For power-ratios lower than the optimum, the growth of ΔSNR evolves slower with lower κ, whereas the opposite is true for power-ratios larger than the optimum. Setting a maximum SNR penalty of 0.2 dB, note that a PR reduction of up to ~ 2.5 dB is tolerated by $\kappa = 0.25$, whereas only ~ 0.5 dB of PR reduction is tolerated by $\kappa = 0.75$.

Note that, although from the B2B perspective it does not make sense to tune the PR, for signal propagation in fiber reducing the PR can be an effective countermeasure for the mitigation of nonlinear effects, as it allows to reduce the power of the higher-cardinality PAM. With the same objective of reducing nonlinear impairments, it has also been shown that PI can play an important role on the performance of TDHMF [11], as it balances the distribution of optical power over time (see Fig. 1). In contrast with TDHMF, the distribution of optical power is inherently constant over time for Flex-PAM. However, it suffers from power unbalance between polarization tributaries, which can only be solved through PI for the $\kappa = 0.5$ case (see Fig. 2). In the remaining cases ($\kappa = 0.25$ and $\kappa = 0.75$) it is not possible to avoid optical power unbalance by simply rearranging the PAM formats among the four quadratures. In that case, a possible way of counteracting polarization unbalance is by reducing the PR, thereby incurring into the B2B penalty shown in Fig. 4. The relationship between the quadrature power-ratio, PR, and the polarization power-ratio, $\mathrm{PR_{pol}}$, is illustrated in Fig. 5 for the different Flex-PAM configurations. Note that $\mathrm{PR_{pol}}$ will not depend on M, but only on PR. It is also worth emphasizing that, similarly to the behavior depicted in Fig. 4, any changes on the polarization power-ratio are less sensitive for $\kappa = 0.25$. Note that, while $\mathrm{PR_{pol}}$ decreases with decreasing PR at a rate of $\sim$0.7 dB/dB for $\kappa = 0.75$, there is only $\sim$0.2 dB of $\mathrm{PR_{pol}}$ variation for $\mathrm{PR} \in [5\ 6]$ dB. Fig. 4 also shows that PI can completely avoid the polarization power unbalance for the case of $\kappa = 0.5$, regardless of the quadrature PR.

This B2B analysis will be particularly useful for the interpretation of the signal propagation performance results introduced in the following section.

III. Results

In a previous work [11], we have shown that the propagation performance of TDHMF can be significantly improved by applying simple countermeasures, such as PI and electronic pre-distortion, for the mitigation of nonlinear impairments. In

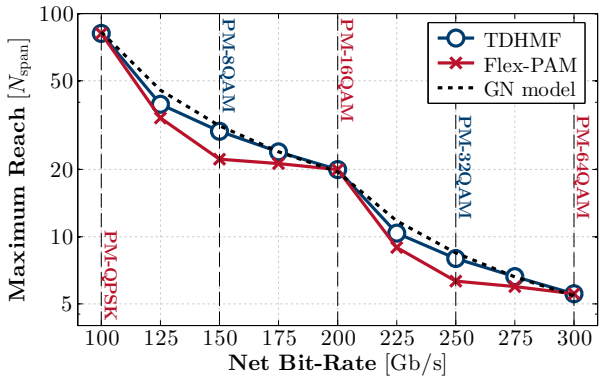

Fig. 6. Maximum reach achieved by TDHMF and Flex-PAM for different bit-rates ranging from 100G to 300G without any nonlinear mitigation countermeasures. Note that both PM-8QAM and PM-32QAM are indicated in the figure only as equivalent spectral efficiency solutions for 150G and 250G.

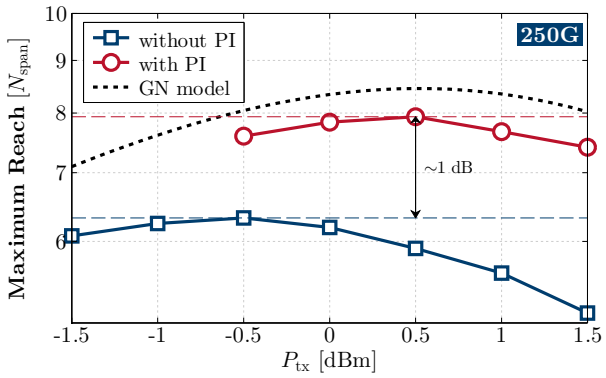

Fig. 7. Maximum reach versus launched power per channel for Flex-PAM at 250G ($\kappa = 0.5$), with and without PI.

this section, we aim to perform and in-depth assessment of the nonlinear propagation performance of both TDHMF and Flex-PAM in uncompensated amplified links, for an extended set of channel net bit-rates, ranging from 100G up to 300G. It is important to remark that, on the contrary of [11], no electronic pre-distortion is applied in this work, with the aim to avoid extra processing complexity both at the transmitter and receiver sides.

The simulation setup is based on the transmission of a 13-Nyquist-WDM channel comb, propagated over a uniform uncompensated and amplified multi-span link, composed of 100 km spans of standard single-mode fiber (SSMF), with attenuation $\alpha = 0.22$ dB/km, dispersion parameter $D = 16.7$ ps/nm/km and nonlinearity coefficient $\gamma = 1.3$ W^{-1}km^{-1}. At the end of each span, the fiber loss is fully recovered by an Erbium-doped fiber amplifier (EDFA) with noise figure of 5 dB. For simplicity, both laser phase noise and frequency-offset are neglected, reducing the receiver-side DSP to a simple least mean squares (LMS) adaptive filter with 51 taps. The net symbol rate per channel is $R_s = 25$ Gbaud, corresponding to a gross symbol rate of 32 Gbaud, including the FEC overhead of 20% and the protocol overhead of 8%. The channel spectra are shaped using a raised-cosine filter with roll-off factor of 0.2. A 50 GHz channel spacing has been set in order to test a state-of-the-art fixed-grid optical link. Targeting the lowest implementation complexity and taking into account the B2B discussion on section II, we have adopted the *same BER* ($\Psi_1 = \Psi_2$) transmitter operation strategy. The power-ratio has been set in accordance to Table I, for a corresponding target BER of 2×10^{-2}.

The first step of our analysis is to evaluate the maximum transmission distance that can be achieved for each considered modulation strategy – TDHMF and Flex-PAM – without applying any countermeasures for nonlinear impairments. The maximum reach is defined in terms of the maximum number of fiber spans, N_{spans}, along which the signal can propagate, while still guaranteeing operation below the defined target BER. Note that the maximum reach is obtained by linear interpolation of the BER results obtained after propagation over a set of transmission distances, thus yielding fractional values of maximum reach in terms of number of spans. In this context, rather than a meaningful propagation distance, these fractional values shall be interpreted as an OSNR margin over the correspondent integer number of spans. For all cases, the maximum reach is determined after optimizing the transmitted power per channel, thus ensuring that the optical signal is being transmitted in the *optimal* propagation regime. The results of this simulation campaign are shown in Fig. 6, in terms of maximum reach versus net channel bit-rate. GN-model [22] predictions are reported as a reference and are based on the B2B SNR requirements derived for each case. As expected, without the implementation of any nonlinear mitigation techniques, both TDHMF and Flex-PAM perform worse than the GN-model predictions due to the power unbalance in time (TDHMF) and in polarization (Flex-PAM). It is also worth noting that Flex-PAM tends to be significantly more penalized, specially for the case of $\kappa = 0.5$, where the polarization power unbalance is highest, as shown in Fig. 5. The higher power level needed by the higher cardinality format generates an extra nonlinear impairment in fiber propagation, compared to a transmission technique based on constant power. Consequently, the maximum reach is significantly reduced with respect to the GN-model predictions. It is important to refer that TDHMF has been tested with a frame composed of only 4 symbols (or 4 time slots), thus approximately reaching its maximum performance. Note that in [11] it has been shown that TDHMF tends to significantly degrade its nonlinear propagation performance with increasing frame-size. Focusing on the Flex-PAM results and considering $M = 2$, we observe a shortening of the maximum reach of about 25% (1.25 dB) for $\kappa = 0.75$, whereas a smaller penalty of approximately 11.5% (0.5 dB) is found for the case of $\kappa = 0.25$. This can be justified by the fact that the polarization power unbalance of Flex-PAM is inherently lower for $\kappa = 0.25$ – approximately 2 dB – as shown in Table I. The same exact pattern can be observed for the case of $M = 4$, but with a reduced penalty: 24% (1.2 dB) and 9.5% (0.4 dB) for $\kappa = 0.75$ and $\kappa = 0.25$, respectively. Again, this slight penalty reduction is well matched with the correspondent reduction of PR_{pol} in Table I from $M = 2$ to $M = 4$. It therefore becomes apparent that polarization power unbalance plays a critical role on the

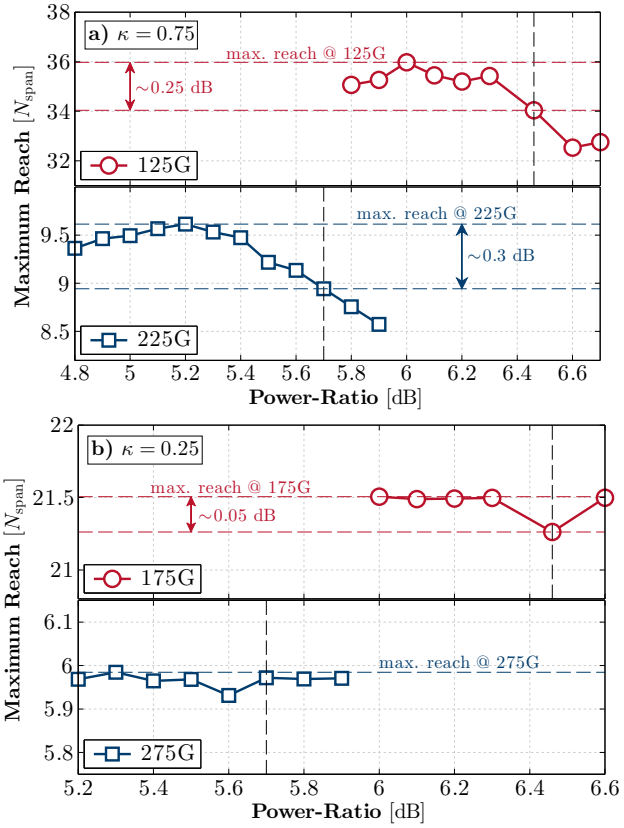

Fig. 8. Power-ratio tuning of Flex-PAM for a) $\kappa = 0.75$ (125G and 225G) and b) $\kappa = 0.25$ (175G and 275G).

nonlinear propagation performance of Flex-PAM.

In order to counteract polarization unbalance, we have then applied the PI technique, which has been firstly proposed for TDHMF [13], [18] to mitigate optical power unbalance over time. The impact of PI on Flex-PAM, can be observed in Fig. 7, which shows the maximum reach versus transmitted power per channel, P_{tx}, at 250G net bit-rate. The advantage of PI is clearly visible, enabling approximately 1 dB (∼20%) improvement both in terms of reach extension and optimal power reduction. Such a behavior confirms that a significant mitigation of nonlinear propagation effects can be achieved by simply balancing the power on the two polarizations. Similar results were also obtained for 150G net bit-rate, which shares the property of $\kappa = 0.5$, required to apply PI in Flex-PAM.

However, as previously stated, for all other bit-rates at which the Flex-PAM is set to operate, where $\kappa \neq 0.5$, PI can not be applied. For those specific cases, we assessed an alternative approach to mitigate the extra nonlinear impairments caused by the polarization power unbalance, which is based on a fine tuning of the PR [21] with respect to the theoretical B2B prescriptions, taking advantage of the PR versus $\mathrm{PR}_{\mathrm{pol}}$ dependence shown in Fig. 5. Although its B2B behavior is easy to predict, the effectiveness of this technique for reach extension must be numerically tested, as the power balancing benefits must overcome the associated SNR penalty experienced by moving from the optimal working point, as shown in Fig. 4. The corresponding maximum reach results

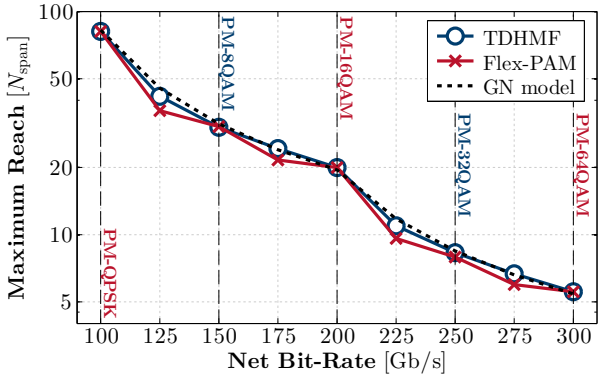

Fig. 9. Maximum reach achieved by TDHMF and Flex-PAM for different bit-rates ranging from 100G to 300G when applying nonlinear mitigation countermeasures: PI and PR tuning. Note that both PM-8QAM and PM-32QAM are indicated in the figure only as equivalent spectral efficiency solutions for 150G and 250G.

obtained for κ =0.75 and κ =0.25 after PR tuning are depicted in Fig. 8, in which we can identify two clearly distinct operation regions:

i) For the $\kappa = 0.75$ case (125G and 225G), an improvement of $\sim$ 0.25–0.3 dB in maximum reach has been achieved by reducing the PR up to $\sim$ 0.4–0.5 dB. However, further reducing the PR generates in an increasing penalty. This trade-off is tightly intertwined with the PR-dependence of B2B performance and polarization power-ratio, as previously discussed on the commenting of Figs. 4 and 5. The benefit of nonlinear mitigation triggered by reducing $\mathrm{PR}_{\mathrm{pol}}$ tends to be the dominant effect for small PR reduction, whereas the fast increase of B2B SNR penalty becomes the leading effect for larger PR reduction.

ii) For the $\kappa = 0.25$ case (175G and 275G), there is no significant improvement in maximum reach brought by PR tuning. As shown in Figs. 4 and 5, the benefit of the slowly decreasing $\mathrm{PR}_{\mathrm{pol}}$ tends to cancel out with the slowly increasing SNR penalty in B2B. In practice, improved nonlinear performance is being traded-off by higher B2B SNR penalty, in such a way that the system performance tends to remain constant.

The overall effectiveness of the considered nonlinear mitigation countermeasures is summarized in Fig. 9, which shows the maximum reach versus net bit-rate for the two hybrid modulation techniques including nonlinear impairments' countermeasures. The GN-model predictions are again plotted as a performance benchmark. A direct comparison with the results of Fig. 6 reveals that all cases based on hybrid modulation formats get an improvement in maximum reach due to the reduction of nonlinear effects, thanks to either PI or PR tuning. For TDHMF, PI allows to almost completely nullify the maximum reach shortening with respect to the GN-model predictions for all tested bit-rates. It is also clear that PI is similarly effective for Flex-PAM when applicable, i.e, for $\kappa = 0.5$. Finally, for Flex-PAM with $\kappa = 0.75$ and $\kappa = 0.25$ it is shown that PR tuning can partially shorten the gap to the GN-model predictions. It is worth of emphasizing that, even if PR tuning is less effective for

$\kappa = 0.25$, its associated reach reduction is significantly lower than that of $\kappa = 0.75$, regardless of the constellation size, due to a lower polarization power unbalance. Consequently, Flex-PAM is generally less impaired by nonlinearities for $\kappa = 0.25$. After applying PI and PR tuning to Flex-PAM, the obtained reach reduction compared to the GN-model predictions is less than 3% for $\kappa = 0.5$, 10% for $\kappa = 0.25$ and 20% for $\kappa = 0.75$.

Finally, it is worth mentioning that although further performance improvement could be obtained by digital nonlinear compensation, in this paper we have focused on the design of simple techniques that do not require any DSP overhead for nonlinear mitigation.

IV. Conclusions

Bit-rate flexibility is a key feature for future optical transponders, in order to allow an efficient use of spectral resources in meshed networks with fast-varying traffic demand. We have theoretically and numerically compared back-to-back and signal propagation performances of two promising flexible modulation techniques: TDHMF and Flex-PAM. Building upon the well-known TDHMF technique, which exploits time-varying modulation, we propose and numerically assess the Flex-PAM concept, which allows integer bit-per-symbol granularity resorting to hybrid PAM modulation among the four orthogonal quadratures in dual-polarization optical signals.

The numerical simulation analysis has revealed that, whereas from the B2B perspective TDHMF and Flex-PAM are shown to be equivalent for integer bit-per-symbol granularity, their signal propagation performance is dominated by rather different nonlinear phenomena, associated with the specificities of their different frame structures. Polarization interleaving is shown to be a simple and effective nonlinear impairment countermeasure for TDHMF and also for Flex-PAM with 50% frame-ratio. Given the impossibility of applying PI to Flex-PAM with 25% and 75% frame-ratio, we assessed a simple power-ratio tuning procedure, which was shown to reduce the power unbalance between polarizations, thereby mitigating nonlinearities. Although the PR tuning was only found to be partially effective for the case of 75% frame-ratio, it was also shown that the nonlinear penalty incurred at 25% frame-ratio is inherently smaller, owing to its correspondent Flex-PAM frame structure. From a general system performance perspective, both TDHMF and Flex-PAM were shown to approach the GN-model predictions in terms of maximum signal reach, incurring into small penalties, provided that the appropriate nonlinear propagation countermeasures are applied. Flex-PAM is shown to be an interesting alternative to the widely studied TDHMF, providing bit-rate flexibility without requiring time-dependent modulation.

Acknowledgments

This work was partially supported by the European Commission through a Marie Skłodowska-Curie individual fellowship, project Flex-ON (653412), and by the GARR Consortium through the "Orio Carlini" 2014 grant.

References

[1] (2015, May) Cisco visual networking index: Forecast and methodology, 2014–2019. Cisco Systems.

[2] G. Wellbrock and T. Xia, "How will optical transport deal with future network traffic growth?" in *Proc. European Conference on Optical Communication (ECOC)*, paper Th.1.2.1, 2014.

[3] Z. Jia, H.-C. Chien, J. Zhang, Y. Cai, and J. Yu, "Performance comparison of dual-carrier 400G with 8/16/32-QAM modulation formats," *IEEE Photon. Technol. Lett.*, vol. 27, no. 13, pp. 1414–1417, July 2015.

[4] J. Fischer, S. Alreesh, R. Elschner, F. Frey, M. Nolle, C. Schmidt-Langhorst, and C. Schubert, "Bandwidth-variable transceivers based on four-dimensional modulation formats," *J. Lightw. Technol.*, vol. 32, no. 16, pp. 2886–2895, Aug 2014.

[5] J. Renaudier, O. Bertran-Pardo, A. Ghazisaeidi, P. Tran, H. Mardoyan, P. Brindel, A. Voicila, G. Charlet, and S. Bigo, "Experimental transmission of Nyquist pulse shaped 4-D coded modulation using dual polarization 16QAM set-partitioning schemes at 28 Gbaud," in *Proc. Optical Fiber Communication Conf. and Exposition (OFC)*, paper OTu3B.1, 2013, pp. 1–3.

[6] L. Beygi, E. Agrell, J. Kahn, and M. Karlsson, "Rate-adaptive coded modulation for fiber-optic communications," *J. Lightw. Technol.*, vol. 32, no. 2, pp. 333–343, 2014.

[7] E. L. T. de Gabory, T. Nakamura, H. Noguchi, W. Maeda, S. Fujita, J. Abe, and K. Fukuchi, "Experimental demonstration of the improvement of system sensitivity using multiple state trellis coded optical modulation with QPSK and 16QAM constellations," in *Proc. Optical Fiber Communications Conference and Exhibition (OFC)*, paper W3K.3, 2015.

[8] G. H. Gho and J. M. Kahn, "Rate-adaptive modulation and low-density parity-check coding for optical fiber transmission systems," *IEEE/OSA Journal of Optical Communications and Networking*, vol. 4, no. 10, pp. 760–768, 2012.

[9] W.-R. Peng, I. Morita, and H. Tanaka, "Hybrid QAM transmission techniques for single-carrier ultra-dense WDM systems," in *16th Opto-Electronics and Communications Conference (OECC)*, 2011, pp. 824–825.

[10] D. van den Borne and S. L. Jansen, "Dynamic capacity optimization using flexi-rate transceiver technology," in *Proc. 17th Opto-Electronics and Communications Conference (OECC)*, 2012, pp. 769–770.

[11] V. Curri, A. Carena, P. Poggiolini, R. Cigliutti, F. Forghieri, C. R. Fludger, and T. Kupfer, "Time-division hybrid modulation formats: Tx operation strategies and countermeasures to nonlinear propagation," in *Proc. Optical Fiber Communication Conf. and Exposition (OFC)*, paper Tu3A.2, 2014.

[12] X. Zhou and L. E. Nelson, "400G WDM transmission on the 50 GHz grid for future optical networks," *J. Lightw. Technol.*, vol. 30, no. 24, pp. 3779 –3792, 2012.

[13] H. Sun, R. Egorov, B. Basch, J. McNicol, and K.-T. Wu, "Comparison of two modulation formats at spectral efficiency of 5 bits/dual-pol symbol," in *Proc. 39th European Conf. Optical Communication (ECOC)*, paper Th.2.D.3, 2013.

[14] X. Zhou, L. Nelson, R. Isaac, P. Magill, B. Zhu, P. Borel, K. Carlson, and D. Peckham, "12,000km transmission of 100GHz spaced, 8×495-Gb/s PDM time-domain hybrid QPSK-8QAM signals," in *Proc. Optical Fiber Communication Conf. and Exposition (OFC)*, paper OTu2B.4, 2013.

[15] X. Zhou, L. Nelson, and P. Magill, "Rate-adaptable optics for next generation long-haul transport networks," *IEEE Commun. Mag.*, vol. 51, no. 3, pp. 41–49, 2013.

[16] Q. Zhuge, M. Morsy-Osman, X. Xu, M. Chagnon, M. Qiu, and D. Plant, "Spectral efficiency-adaptive optical transmission using time domain hybrid QAM for agile optical networks," *J. Lightw. Technol.*, vol. 31, no. 15, pp. 2621–2628, 2013.

[17] Q. Zhuge, X. Xu, M. Morsy-Osman, M. Chagnon, M. Qiu, and D. Plant, "Time domain hybrid QAM based rate-adaptive optical transmissions using high speed DACs," in *Proc. Optical Fiber Communication Conf. and Exposition (OFC)*, paper OTh4E.6, 2013.

[18] R. Rios-Muller, J. Renaudier, O. Bertran-Pardo, A. Ghazisaeidi, P. Tran, G. Charlet, and S. Bigo, "Experimental comparison between Hybrid-QPSK/8QAM and 4D-32SP-16QAM formats at 31.2 GBaud using Nyquist pulse shaping," in *Proc. 39th European Conf. Optical Communication (ECOC)*, paper Th.2.D.2, 2013.

[19] R. Li, P. Cortada, V. Curri, and A. Carena, "Flex -PAM modulation formats for future optical transmission system," in *Fotonica AEIT Italian Conference on Photonics Technologies*, 2015.

[20] R. Li, V. Curri, and A. Carena, "Bit-rate maximization for elastic transponders operating in WDM uncompensated amplified links," in *Proc. Optical Fiber Communication Conf. and Exposition (OFC)*, paper Th2A.45, 2016.
[21] F. Buchali, L. Schmalen, K. Schuh, and W. Idler, "Optimization of time-division hybrid-modulation and its application to rate adaptive 200Gb transmission," in *Proc. 40th European Conf. Optical Communication (ECOC)*, 2014.
[22] P. Poggiolini, G. Bosco, A. Carena, V. Curri, Y. Jiang, and F. Forghieri, "The GN-model of fiber non-linear propagation and its applications," *J. Lightw. Technol.*, vol. 32, no. 4, pp. 694–721, 2014.
[23] I. A. Glover and P. M. Grant, *Digital Communications*, 3rd ed. Prentice Hall, 2009.